Int. J. Environ. Sci. Technol. (2018) 15:2337–2348
https://doi.org/10.1007/s13762-017-1603-9

ORIGINAL PAPER

Carbon steel slag and stainless steel slag for removal of arsenic from stimulant and real groundwater

W. Shi[1] · H. Li[2] · G. Liao[2] · G. Pei[2] · Y. Lin[3]

Received: 9 March 2017 / Revised: 4 October 2017 / Accepted: 10 October 2017 / Published online: 22 October 2017

Abstract Arsenic in groundwater is a serious environmental problem. The contamination of groundwater with arsenic has been of utmost concern worldwide. Steel slag is a solid waste generated from steel production. Although steel slags have been used for arsenic removal from water, this process has not been systematically or integratively researched. In this study, the arsenic removal capacity and mechanism were investigated for carbon steel slag, stainless steel slag and Fe-modified stainless steel slag based on an in-depth study. The study also evaluated the potential utilization of different steel slag for regeneration. The maximum adsorption of arsenic on carbon steel slag, stainless steel slag and Fe-modified stainless steel slag was 12.20, 3.17 and 12.82 mg g^{-1} at 25 °C, respectively. The modification of stainless steel slag by $FeC1_3$ can generate more pore structures and larger surface areas, and 300 °C treatment produces the best regeneration efficiency. The ΔG values were negative for all of the steel slags, indicating the spontaneous nature of the adsorption process. The solution pH was a critical parameter for the removal of arsenic for steel slags. Under highly alkaline solution conditions, the mechanism of arsenic removal by carbon steel slag and stainless steel slag can be attributed to chemisorption, including chemical precipitation and coordination reactions, and under weakly alkaline solution conditions, electrostatic interaction and specific adsorption are the arsenic removal mechanisms by Fe-modified stainless steel slag. Regeneration of the Fe-modified stainless steel slag was better achieved than that of the other steel slags in the application of high-temperature treatment.

Keywords Arsenic pollution · Groundwater remediation · Modification · Regeneration experiment · Steel slag

Editorial responsibility: V.K. Gupta.

Electronic supplementary material The online version of this article (doi:10.1007/s13762-017-1603-9) contains supplementary material, which is available to authorized users.

✉ W. Shi
shiweiyu@swu.edu.cn

[1] Chongqing Key Laboratory of Karst Environment, School of Geographical Sciences, Southwest University, Chongqing 400715, China

[2] School of Environmental Science and Resources, Shanxi University, Taiyuan 030006, Shanxi, China

[3] Department of Civil and Environmental Engineering, Northeastern University, Boston, MA 02115, USA

Introduction

Water is considered as the elixir of life because the world would not have any life without water. The amount of waste water is increasing with the rapid growth of industrialization (Rajendran et al. 2016). Water pollution creates major environmental issues around the globe. Hence, pollution treatment should be a major concern. Several methods and technologies have been developed for the treatment of waste water, including photocatalyst (Saravanan et al. 2015), ultrasonic waves (Dastkhoon et al. 2015; Nikfar et al. 2016), reverse osmosis (Saravanan et al. 2013a), adsorption (Gupta et al. 2015; Nekouei et al. 2015; Robati et al. 2016) and degradation (Saravanan et al. 2013b, c). In particular, nanomaterials are also important for the removal of pollutant in the aqueous materials (Saravanan et al. 2011, 2014; Asfaram et al. 2015; Gupta et al. 2017).

Arsenic (As) is a contaminant of international concern due to its toxicity and carcinogenicity. The long-term

uptake of As causes various diseases, such as hyper-pigmentation, conjunctivitis, liver cancer, lung cancer and skin cancer (Yang et al. 2014). Arsenic in groundwater is a serious environmental problem. The contamination of groundwater with arsenic has been of utmost concern across the world (Biswas et al. 2014). It has been observed in many countries of the world, such as the USA, China, Chile, Argentina, Poland, Canada, Hungary, New Zealand, Japan and India. In the north Shanxi province of China, the problem is severe (Wang et al. 2004), as drinking water is drawn mainly from groundwater for many humans in this region (Luo et al. 2014). The World Health Organization (WHO) has reported the As maximum contaminant level (MCL) in drinking water as between 10 and 50 μg L^{-1}. Therefore, it is necessary to remove As from water.

Several methods, such as filtration (Wickramasinghe et al. 2004), adsorption (Kim et al. 2012; Essandoh et al. 2017), coagulation–flocculation (Sun et al. 2013), ion exchange (Jia et al. 2013) and membrane technology (Chakrabortty et al. 2014), have been used for As removal. For these methods or technologies, adsorption has been the most widely applied because it is simple, effective and economically feasible. Although metal oxides and hydroxides of iron or alumina are considered the most common adsorbents for As removal from water (Kanel et al. 2006), these adsorbents may not be the optimal selection considering local conditions and sustainability. Therefore, an agent or material with a low cost needs to be developed to remove As from groundwater considering the local conditions. Shanxi province is one of the most important heavy industrial bases of China. Large amounts of industrial waste are produced every year, and steel slag is a prominent industrial waste for this region. Developing steel slag as an agent for removal of As from water would improve local water safety and resource recycling.

Steel slag is a solid waste generated from steel production. In the steelmaking process, the two main slag types are identified as blast furnace slag and steel slag (Claveau-Mallet et al. 2013). Blast furnace slag is produced from the conversion of iron ore into pig iron, and steel slag is produced as the pig iron is purified into steel. Based on the type of steel, steel slag can also be divided into carbon steel slag and stainless steel slag. The steel slag mainly consists of iron oxides and calcium hydroxides. The iron oxides can adsorb anions such as As, Cr, Cu and P (Oh et al. 2012; Claveau-Mallet et al. 2013), and calcium hydroxides can increase the microenvironmental pH and then promote the precipitation of dissolved heavy metal cations (Ahn et al. 2003).

Further, using steel slag to remove As in water has been investigated. Chakraborty et al. (2014) provided an adsorption experiment for arsenic removal from contaminated groundwater with an emphasis on the influence of steel slag composition. Oh et al. (2012) investigated mechanisms for removing arsenic and studied its re-leaching process in simulating acidic aqueous solution. Ahn et al. (2003) compared the removal efficiency of arsenic from mine tailing leachate using different steel manufacturing byproducts and inferred the removal mechanisms. Although the previous studies focused on different aspects of As removal using steel slag, the concept itself has not been systematically or integratively researched.

The objectives of the present study are to (1) compare the capacity of carbon steel slag (CSS), stainless steel slag (SSS) and Fe-modified stainless steel slag (Fe-SSS) for removal of As from synthetic groundwater; (2) investigate the influence and mechanism of As removal on the adsorption kinetics based on batch experiments; and (3) evaluate the potential utilization of steel slag regeneration. Present research was conducted in 2012, in the Environmental Remediation Laboratory of School of Environmental Science and Resources, Shanxi University, Taiyuan, Shanxi, China.

Materials and methods

Characters and modification of materials

Both the carbon steel slag and the stainless steel slag used in this study were obtained from Taiyuan Iron and Steel (Group) Co., Ltd., Taiyuan, Shanxi. China. Both samples were ground, sieved to pass through a 100-mesh sieve (0.15 mm) and then dried at 105 ± 0.5 °C for 4 h and cooled to ambient temperature in a desiccator for analysis and use in the experiment.

According to the current study, As removal by stainless steel slag is not sufficient to meet drinking water standards. Therefore, stainless steel slag was defined as the original sample for $FeC1_3$ solution modification. Modified steel slag was prepared.

The original sample was soaked in 0.2, 0.5, 0.8, 1.0, 1.2 and 1.5 mol L^{-1} FeC13 solution and shaken in the shaker at 160 rpm for 24 h at room temperature (25 °C); then, the precipitate was collected by centrifuge at 4000 rpm for 10 min and washed in deionized water to neutrality (pH 6.5–7.5). Finally, the sample was heated at 110 °C for 24 h and then sealed in the desiccator for use.

The morphological characteristics of the samples were obtained by scanning electron microscopy (SEM) (S-4800, Hitachi, Japan). The main chemical compositions of the samples were measured using an X-ray fluorescence (XRF) spectrometer (PW2424, Philips, Netherlands). X-ray diffraction (XRD) patterns of the samples were recorded by

an X'Pert PRO system (PANalytical, Netherlands) in the diffraction angle (2 h) range of 5°–70°.

Batch experiment on As removal from synthetic solution

Adsorption kinetics and batch equilibrium were investigated using a short-term batch experiment. Synthetic solutions were prepared with deionized water and a standard solution of As_2O_3 (GSB 07-1275-2000, China). Before both of the experiments, optimum parameters, including particle size and shaker speed, were obtained.

To find an optimal adsorbent dosage, experiments were conducted at 10, 16, 20, 24, 30, 36 and 40 g L^{-1} adsorbent dosages for 3 h, with an initial As ion concentration of 0.2 mg L^{-1} and a solution pH of 10.0 ± 0.5.

Adsorption kinetics study: In this portion of the study, 1.00 g of steel slag with a 100-mesh sieve (0.15 mm) was added to each conical flask with an As concentration of 0.2 mg L^{-1}. The flasks were shaken in the shaker at 160 rpm under alkaline conditions (pH = 10 ± 0.5) at room temperature (25 °C) for different contact times (5, 15, 25, 30, 45 and 60 min). At the end of the experiment, a 1-mL solution was collected and centrifuged at 5000 rpm for 5 min. The filtrate was collected in polythene tubes and diluted before analysis. Every treatment was conducted in triplicate. The amount of As adsorbed per unit of adsorbents at time t, q_t (mg g^{-1}), was calculated by

$$q_t = \frac{(C_0 - C_t)V}{m} \tag{1}$$

where C_0 and C_t are the concentrations of As initially and after time t (mg L^{-1}), respectively; V is the volume of the solution (L); and m is the amount of adsorbent used (g).

The adsorption kinetics of As were analyzed by applying three typical kinetic models, including the Lagergren pseudo-first-order equation (Lagergren 1898):

$$\ln(q_e - q_t) = \ln q_e - k_1 t \tag{2}$$

pseudo-second-order adsorption kinetics equations (Duan and Su 2014):

$$\frac{t}{q_t} = \frac{1}{k_2 q_e^2} + \frac{t}{q_e} \tag{3}$$

and the intra-particle diffusion kinetic equation (Weber and Morris 1963):

$$q_t = k_i t^{0.5} + C \tag{4}$$

where q_e and q_t are the adsorption capacity of the adsorbent (mg L^{-1}) at equilibrium and contact time t (minutes); k_1, k_2 and k_i are the rate constants of the pseudo-first-order, pseudo-second-order and intra-particle diffusion equations, respectively; and C is the intercept, which is proportional to the extent of boundary layer thickness.

Effects of initial solution pH: The effects of the initial solution pH (3.0, 5.0, 7.0, 9.0 and 11.0) on the As adsorption were evaluated using a batch adsorption process under the following conditions: reaction temperature of 25 °C; adsorbent dosage of 1.0 g; initial As(III) concentration of 0.2 mg L^{-1}; and contact time of 3 h. The pH values and As concentrations of the solutions were measured immediately after placing the adsorbent into the solution (initial pH), and after reaction equilibrium was reached (final pH). The amount of As adsorbed was also calculated by Eq. (1).

Batch equilibrium studies: A series of 250-mL conical flasks were filled with solutions with different initial As concentrations (0.05, 0.1, 0.2, 0.5, 1.0 and 2.0 mg L^{-1}). Then, 1.00 g of steel slag passing through a 100-mesh sieve (0.15 mm) was added into each conical flask. The flasks were also shaken in the shaker at 160 rpm under alkaline conditions (pH = 10 ± 0.5) at room temperature (25 °C). After the optimum uptake time (30 min), the concentrations of As were calculated by taking the difference in the initial and equilibrium concentrations. The amount of adsorbed As at equilibrium, q_e (mg g^{-1}), was calculated according to the following equation:

$$q_e = \frac{(C_0 - C_e)V}{m} \tag{5}$$

where C_0 is the initial As concentration (mg L^{-1}) and C_e is the equilibrium As concentration (mg L^{-1}).

The experimental data were analyzed using the Langmuir (1918) and Freundlich and Heller (1939) isotherm models. These isotherm models can be formulated as follows:

$$\frac{C_e}{q_e} = \frac{1}{b \cdot q_m} + \frac{C_e}{q_m} \tag{6}$$

$$q_e = K_f \cdot C_e^{\frac{1}{n}} \tag{7}$$

where C_e (mg L^{-1}) and q_e (mg g^{-1}) are the equilibrium adsorbate concentrations in the aqueous and solid phases, q_m is the maximum adsorption capacity of the adsorbent (mg g^{-1}), b is the Langmuir adsorption constant (L mg^{-1}), and K_f and n are the Freundlich equilibrium constants related to adsorption capacity and adsorption intensity, respectively.

The Gibbs free energy change was also calculated based on Eq. (8) (Ajmal et al. 1998):

$$\Delta G = -RT \ln b \tag{8}$$

where ΔG is the Gibbs free energy change, R is the universal gas constant (8.314 J mol^{-1} K^{-1}), T is the absolute temperature (K), and b is the Langmuir constant (L mol^{-1}).

All the experiments were carried out in triplicate, and the data were expressed as the average value with standard deviation values.

Regeneration experiment from real As-contaminated groundwater

Using real As-contaminated groundwater, after the adsorption and equilibrium process, the As-saturated CSS and Fe-SSS were treated separately with NaOH and high temperature to determine regeneration. The samples of real groundwater were taken from Shanyin County, Shuozhou City, North of Shanxi province, China. The As concentration in real groundwater was 153 μg L^{-1}.

NaOH treatment: The As-saturated sample was soaked in 0.05, 0.1, 0.2, 0.4, 0.8 and 1.0 mol L^{-1} NaOH liquor and shaken in the shaker at 160 rpm for 24 h at room temperature (25 °C); then, the precipitate was collected by centrifuging at 4000 rpm for 10 min and was washed in deionized water to neutrality (pH 6.5–7.5). Finally, the washed precipitate was heated at 110 °C for 24 h and then sealed in the desiccator for use.

High temperature: The As-saturated samples were treated at 200, 300, 400 and 500 °C in a heat-resistant furnace for 60 min, cooled to room temperature (25 °C) and then sealed in the desiccator for use.

According to the comparison of the two regeneration methods, the 300 °C high-temperature regeneration was selected. Then, the optimal treatment time experiment was conducted at different heating times (15, 30, 60 and 90 min) at 300 °C. After the optimal treatment time experiment, the regeneration experiment was carried out 5 times under optimal conditions.

Determination of total As concentration

Working standard solutions were prepared by appropriate stepwise dilution of a 1000 mg L^{-1} stock standard solution of As_2O_3 (GSB 07-1275-2000, China) just before use. The reducing agent was a 2% (w/v) sodium tetrahydroborate solution that was stabilized with 0.5% (w/v) sodium hydroxide. It was also prepared daily using analytical-grade reagents and was filtered through a 0.45-μm filtration membrane. The 10% (w/v) potassium iodide solution in 2% (w/v) ascorbic acid was prepared by dilution of the reagents with deionized water.

Each plastic container was washed with tap water and a diluted Extran solution, soaked in 10% (v/v) nitric acid solution for 24 h and rinsed three times with deionized water before it was used.

After the batch experiment, the slag suspension was centrifuged at 5000 rpm for 5 min, and the supernatant solution was filtered through a 0.45-μm membrane filter paper. The 5-mL solution was transferred to a 10-mL volumetric flask, with 3.0 mL of 6.0 mol L^{-1} hydrochloric acid and 1.5 mL of 10% (w/v) potassium iodide in 2% (w/v) ascorbic acid solution. After 30 min, the solution was brought to volume with deionized water, and this solution was analyzed for As by atomic fluorescence spectrometry (AFS).

Toxicity tests

Toxicity tests were performed to assess the environmental innocuity of the steel slag. Distilled water used as an extraction fluid was tested according to the Toxicity Characteristic Leaching Procedure (TCLP) (USEPA 1992). This testing methodology is used to determine whether a waste is characteristically hazardous. A 35-g steel slag sample was placed in a 1000-mL Erlenmeyer flask filled with 700 mL of extraction fluid. The sample in the flask was mixed for 24 h, after which metal concentrations were determined. Samples were tested in duplicate, and mean concentrations were reported.

Results and discussion

Results

Chemical composition and toxicity characteristic of different steel slags

Table 1 shows that the main chemical components of the CSS, SSS and Fe-SSS are Fe_2O_3, SiO_2, Al_2O_3, CaO and MgO. CaO represents the largest portion of the different steel slags (over 70% by mass). The Fe_2O_3 content among the three steel slags is highly variable.

Table 1 Chemical composition of carbon steel slag (CSS), stainless steel slag (SSS) and Fe-modified stainless steel slag (Fe-SSS)

Component (%)	Slag ID		
	CSS	SSS	Fe-SSS
SiO_2	10.65	24.74	27.18
Al_2O_3	3.29	2.50	2.99
Fe_2O_3	23.94	0.56	17.59
MgO	9.49	8.41	5.81
CaO	39.94	51.44	29.67
Na_2O	0.04	0.07	0.06
K_2O	0.02	0.02	0.02
MnO	2.29	0.15	0.35
P_2O_5	1.29	0.02	0.05
TiO_2	0.49	0.21	0.33
Cr_2O_3	0.56	0.72	1.45

ND no determination

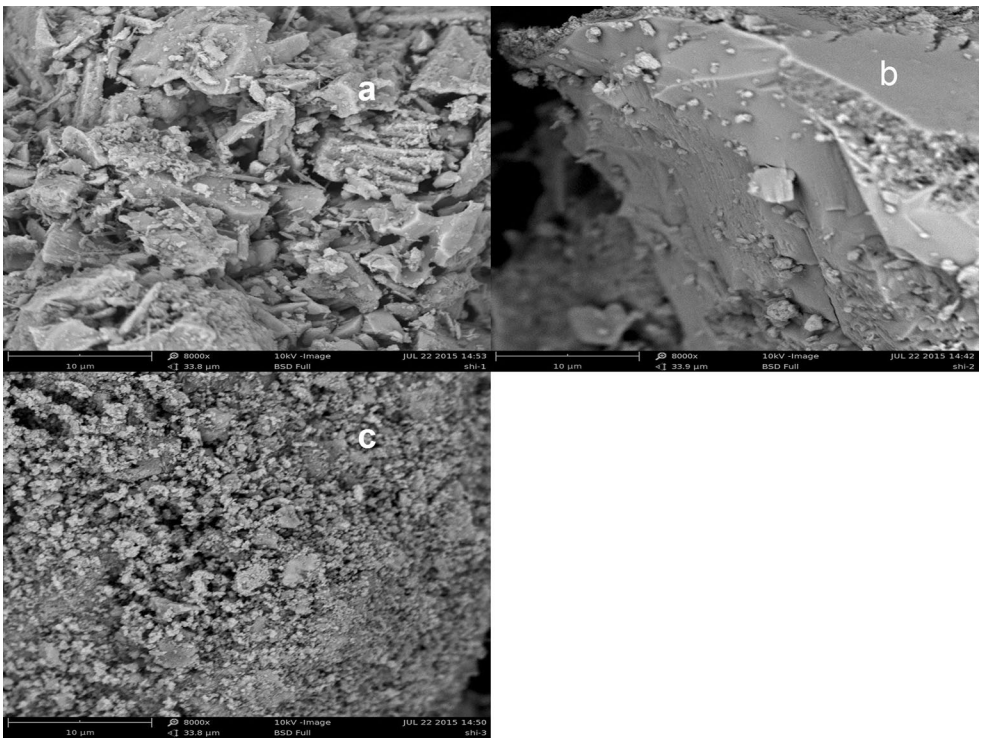

Fig. 1 SEM photographs for surface of **a** carbon steel slag, **b** stainless steel slag and **c** Fe-modified stainless steel slag (× 8000)

The slag surface was examined by SEM analyses. Figure 1 shows the significant differences of surface textures among CSS, SSS and Fe-SSS. The surface of SSS is smooth, while CSS and Fe-SSS have more pores and a coarser surface.

The XRD patterns of the CSS, SSS and Fe-SSS are shown in Fig. 2, which indicates peaks with complex patterns, with some overlapping. CSS, SSS and Fe-SSS contain dicalcium silicate, larnite, fluarite, melanterite and oxide phase (RO).

The environmental safety of the tested slags was evaluated through toxicity tests. The results indicated that the toxicity of the slags was low or below the detection limit of the metal concentrations (Table S1). Nevertheless, the pH value of the three kinds of slags is alkaline, with the pH value of CSS and SSS approximately 12. F was also observed, but in very small quantities.

Effect of contact time and pH

Figure 3 shows the effect of contact time on the adsorption of CSS, SSS and Fe-SSS for As. The adsorption capacity of SSS for As is significantly lower than that for CSS and Fe-SSS. The test also indicated that the saturated As adsorption capacity of CSS is the highest. According to the adsorption kinetics data, three kinetic models, namely pseudo-first-order, pseudo-second-order and intra-particle diffusion models, were applied for analysis (Table 2). The theoretical q_e value of CSS, SSS and Fe-SSS is close to the experimental q_e value (10.356 mg g^{-1} for CSS, 7.763 mg g^{-1} for SSS and 9.105 mg g^{-1} for Fe-SSS). The correlation coefficient of the pseudo-second-order model is the highest among the three models.

Figure 4 shows the effect of initial solution pH on adsorption capacity and final solution pH. Even though the initial solution pH is exceedingly acidic (pH < 3), CSS, SSS and Fe-SSS effectively changed the solution pH and kept the solution pH at approximately 11.9, 11.3 and 9.5, respectively (Fig. 4a). While the adsorption capacity of SSS was affected, the initial solution pH did not significantly affect As adsorption capacity for CSS and Fe-SSS (Fig. 4b).

Effect of adsorbent dosage

The effect of the CSS, SSS and Fe-SSS dosage on the removal of As is shown in Fig. 5. With an increase in the dosage of CSS, SSS and Fe-SSS from 10 to 40 g L^{-1}, the As removal efficiency increased from 85.4, 46.7% and 85.7 to 97.6%, 85.0 and 96.6%, respectively. The As removal

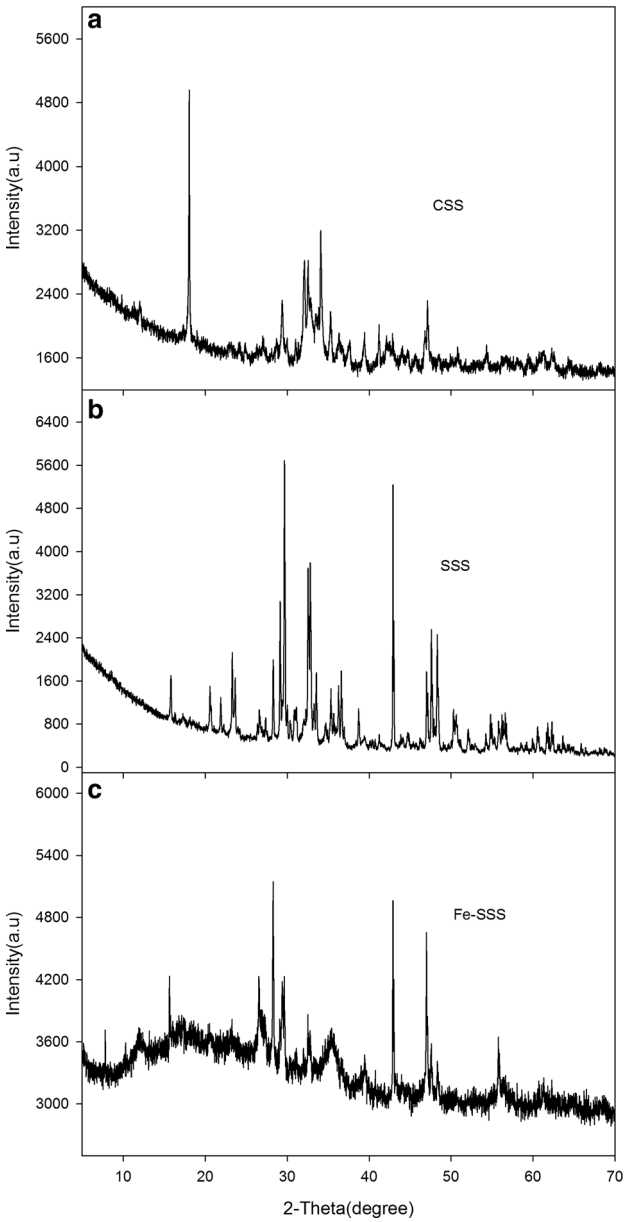

Fig. 2 XRD patterns of **a** carbon steel slag, **b** stainless steel slag and **c** Fe-modified stainless steel slag

efficiency of SSS is significantly lower than that of the others.

The adsorption isotherms of As on CSS, SSS and Fe-SSS are illustrated in Fig. 6. To predict the equilibrium amount of As sorbed onto CSS, SSS and Fe-SSS, the experimental results were fitted to the Langmuir and Freundlich equations (correlation coefficient, $R^2 > 0.90$). Table 3 shows the Langmuir and Freundlich isotherm coefficients. The maximum adsorption of As on CSS, SSS and Fe-SSS calculated by the Langmuir isotherm was 12.20, 3.17 and 12.82 mg g^{-1} at 25 °C, respectively. The Gibbs free energy change (ΔG) for the adsorption of As on CSS, SSS and Fe-SSS is listed in Table S2. The ΔG values were negative for all slags, and the ΔG value of CSS was more negative than the others.

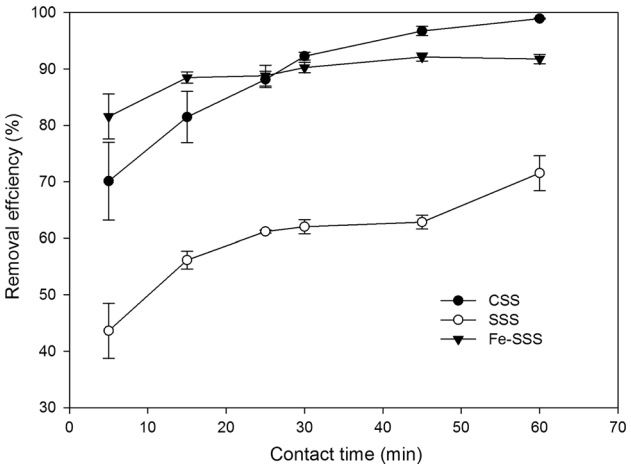

Fig. 3 Kinetics of As(III) adsorption in simulant groundwater for carbon steel slag (CSS), stainless steel slag (SSS) and Fe-modified stainless steel slag (Fe-SSS) at 25 °C; the initial concentration of As(III) is 0.2 mg L^{-1}, and the solution pH is 10.0 ± 0.5

As removal from real groundwater and regeneration of steel slags

Based on the batch experiment, CSS and Fe-SSS performed better for As removal. Therefore, CSS and Fe-SSS were selected and used in a real groundwater experiment. Figure 7a, b shows the As removal efficiency of CSS and Fe-SSS regenerated from As-saturated CSS and Fe-SSS treated with NaOH and high temperature, respectively. With an increase in the NaOH concentration from 0.05 to 3.00 mol L^{-1}, the As removal efficiency on regenerated CSS and Fe-SSS increased from 29.3 and 27.6% to 75.7 and 83.0%. Nevertheless, the As removal efficiency on CSS and Fe-SSS regenerated by high temperature remains steady at 85 and 90% even though the temperature increased. The 300 °C treatment performs regeneration most efficiently.

When the treatment time reached 60 min at 300 °C, the As removal efficiency on CSS and Fe-SSS was optimal at 86.5 and 94.6% (Fig. 7c). Figure 7d indicates that even though regeneration was repeated four times, the As removal efficiency on CSS and Fe-SSS also remained high (86 and 94%).

Table 2 Kinetic parameters for adsorption of As on carbon steel slag (CSS), stainless steel slag (SSS) and Fe-modified stainless steel slag (Fe-SSS)

Sorbent	Pseudo-first-order			Pseudo-second-order			Intra-particle diffusion		
	q_e	$k_1 \times 10^{-2}$	R^2	q_e	$k_2 \times 10^{-2}$	R^2	k_i	C	R^2
CSS	9.960	6.032	0.972	10.377	2.679	0.998	0.528	6.039	0.888
SSS	7.735	4.216	0.667	7.738	2.146	0.975	0.495	3.443	0.872
Fe-SSS	9.117	12.762	0.740	9.083	11.600	0.999	0.175	7.726	0.700

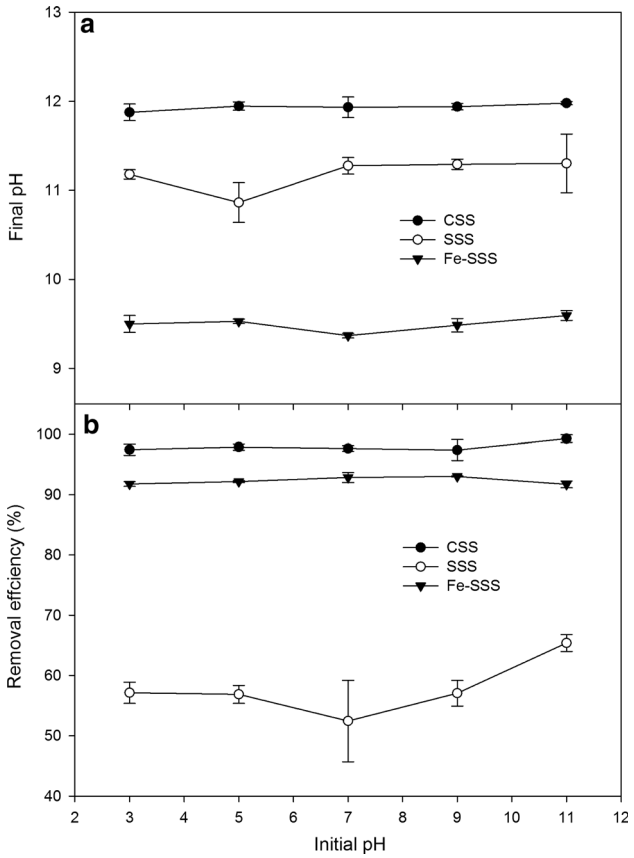

Fig. 4 Effect of initial pH on As(III) adsorption and **a** final pH and **b** removal efficiency for carbon steel slag (CSS), stainless steel slag (SSS) and Fe-modified stainless steel slag (Fe-SSS); reaction temperature: 25 °C; initial As(III) concentration: 0.2 mg L^{-1}; contact time: 3 h

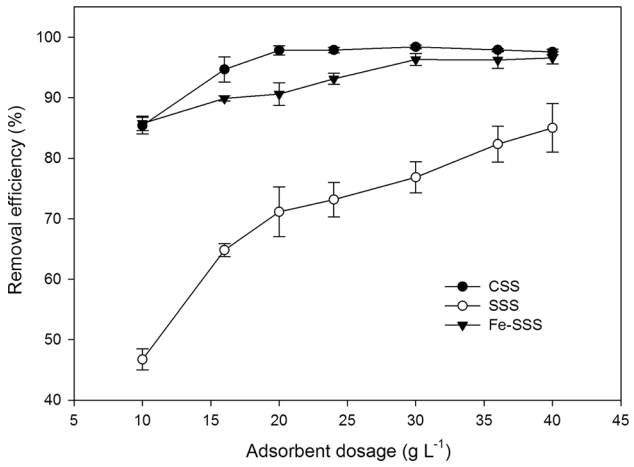

Fig. 5 Effect of dosage of carbon steel slag (CSS), stainless steel slag (SSS) and Fe-modified stainless steel slag (Fe-SSS) on adsorption capacity; reaction temperature: 25 °C; initial As(III) concentration: 0.2 mg L^{-1}; solution pH: 10.0 ± 0.5; contact time: 3 h

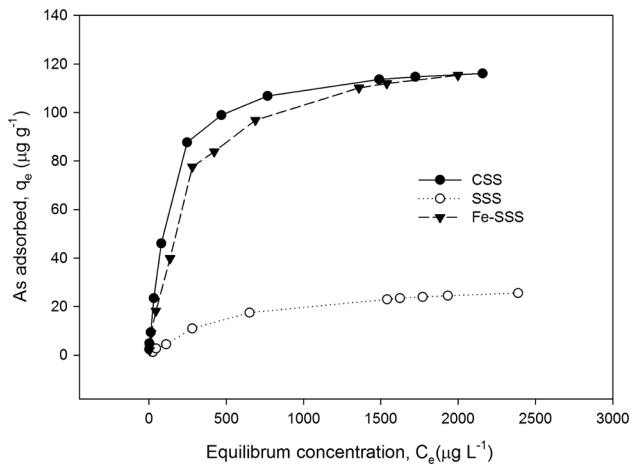

Fig. 6 Adsorption isotherms of As(III) on carbon steel slag (CSS), stainless steel slag (SSS) and Fe-modified stainless steel slag (Fe-SSS). Different initial As(III) concentrations: 0.05, 0.1, 0.2, 0.5, 1.0 and 2.0 mg L^{-1}; initial pH 10 ± 0.5; contact time: 30 min; reaction temperature: 25 °C

Discussion

Arsenic mainly exists in groundwater as arsenite and arsenate [As(V)] species. More attention is required for the removal of As(III) due to its high toxicity and mobility than for that of As(V) (Kanel et al. 2006). Therefore, in the synthetic groundwater experiment, As(III) as the initial As species was studied to understand the removal mechanism of As by different steel slags.

Adsorption kinetics modeling is a classic method that could not only estimate adsorption rates but also lead to suitable rate expression characteristics of a possible

Table 3 Langmuir and Freundlich isotherm parameters for adsorption of As on carbon steel slag (CSS), stainless steel slag (SSS) and Fe-modified stainless steel slag (Fe-SSS) at 25 °C

Sorbent	Langmuir isotherm			Freundlich isotherm		
	q_m (mg g^{-1})	b (L mg^{-1})	R^2	K_f	n	R^2
CSS	12.20	9.18	0.985	1.92	1.42	0.905
SSS	3.17	1.76	0.987	0.16	1.41	0.972
Fe-SSS	12.82	1.49	0.986	0.90	1.27	0.913

reaction mechanism (Donmez et al. 2015). In this study, the pseudo-second-order model was the most suitable for describing the experimental data, which suggests that the chemisorption process could be a rate-limiting step (Ho 2006). The q_e of SSS is lowest among the three slags, which also demonstrated adsorption capacity as the poorest. SEM revealed that CSS and Fe-SSS had more opening of channels, enlargement of aperture diameter and creation of higher microporosity, which suggested a higher surface area resulting in more adsorption sites and chemical reaction position (Fig. 1).

The initial solution pH is one of the most key adsorption parameters. Even though the initial solution was acidic, the CSS, SSS and Fe-SSS regulated it to alkalinity because the three steel slags are alkaline materials that can perform hydration with H_2O and neutralize H^+ with released OH^-

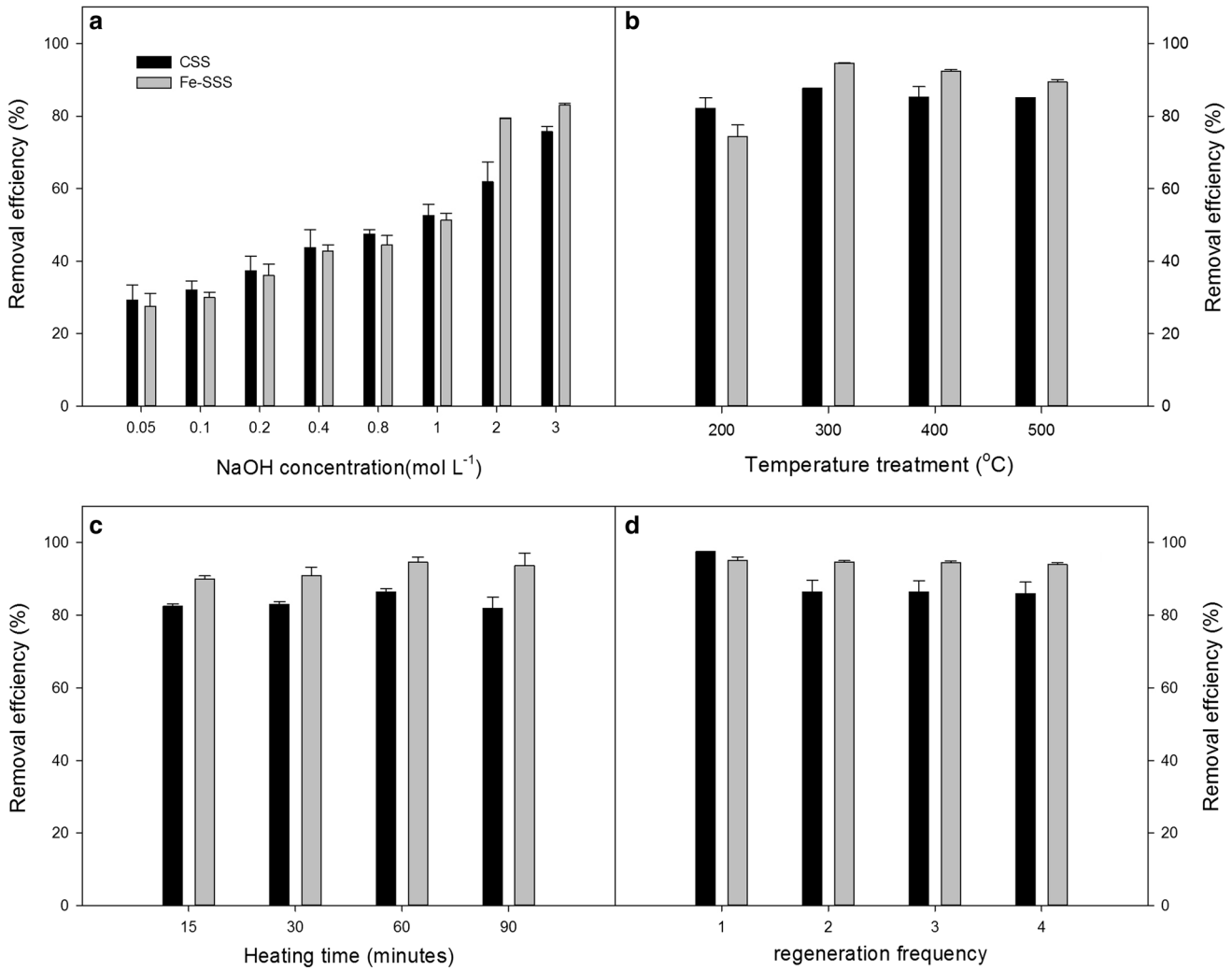

Fig. 7 As removal capacity of carbon steel slag (CSS) and Fe-modified stainless steel slag (Fe-SSS) using **a** different concentration of NaOH treatment for regeneration, **b** different high-temperature treatment for regeneration, **c** different heat time under 300 °C regeneration and **d** 5 cycles of regeneration under 300 °C for 30 min

ions. Oh et al. (2012) found that hydrolysis and ionization of steel slag would react acutely at a lower pH. Duan and Su (2014) suggested that in a strongly acidic medium (pH < 3), a positive charge develops in the surface of steel slag upon consumption of H^+, followed by an increase in pH. The reaction equation is as follows:

$$\text{Sur-OH} + \text{H}^+ \rightarrow \text{Sur-OH}_2^+ \quad (9)$$

where Sur stands for the surface sites of the slag and Sur-OH represents a surface hydroxyl group.

When the pH is greater than 3, a negative charge develops on the surface of steel slag while consuming OH-, as described in this reaction formula:

$$\text{Sur-OH} + \text{OH}^- \rightarrow \text{Sur-O}^- + \text{H}_2\text{O} \quad (10)$$

This reduces the effect of hydration of the slag on the final pH, maintaining the final pH at a stable value.

Generally, anion adsorption would be inhibited under high pH conditions. Nevertheless, under high pH condition (pH > 11), adsorption on CSS and SSS occurred smoothly. That is because arsenic (III) removal by steel slag may also be attributed to the formation of calcium arsenite under high pH conditions (Ahn et al. 2003). The reaction equation is as follows:

$$\text{HAsO}_3^{2-} + \text{Ca}^{2+} + n\text{H}_2\text{O} \rightarrow \text{CaHAsO}_3 \cdot n\text{H}_2\text{O} \quad (11)$$

Dutre and Vandecasteele (1998) demonstrated that formation of $CaHAsO_3$ in the solution led to a decrease in As(III) concentrations due to the presence of $Ca(OH)_2$. Additionally, CaO was determined to be the largest component of steel slags in this study. It could be concluded that the reaction would happen.

However, this explanation is only suitable for high pH conditions on CSS and SSS. Although Fe-SSS could cause the solution pH to maintain low alkalinity, the As removal efficiency of Fe-SSS was much higher than that of SSS. In addition to the increased surface area of Fe-SSS compared with that of SSS, Lackovic et al. (2000) suggested that surface precipitation or adsorption would result in arsenic removal by iron. They indicated that electrostatic interaction and specific adsorption would be key processes for As removal by iron oxides. Because Fe-SSS is rich in iron compared with SSS (Table 1), the As sorption processes are more pronounced. As predominantly forms inner-sphere, bidentate surface complexes with goethite (Cerkez et al. 2015). Grossl et al. (1997) proposed an As adsorption mechanism involving goethite: (1) formation of an inner-sphere, monodentate surface complex through ligand exchange reaction of $H_2AsO_3^-$ or $H_2AsO_4^-$ with goethite; (2) formation of an inner-sphere, bidentate surface complex via a second ligand exchange reaction. That explains why in weakly alkaline condition, Fe-SSS can still perform more efficiently for As removal than SSS.

Additionally, the ΔG values were negative for all of the steel slags, indicating their spontaneous adsorption process. The ΔG of CSS was most negative among the three steel slags. This indicates that the adsorption process is more favorable for CSS compared with other slags at room temperature. That may be caused by the adsorbent surface activation and/or high pore size of the CSS, which was depended on thermodynamic process. The previous study has found the ΔG values were negative at all of the temperatures for adsorption process by steel slag. The values of ΔG become more negative with increasing temperature (Duan and Su 2014). This indicates that the adsorption process becomes more favorable at higher temperatures, which means the increase in temperature will promote adsorption process.

As(III) is the single initial As species in synthetic groundwater, but in the real groundwater, both As(III) and As(V) species are found. In the case of As(V), the main aqueous arsenate species are $HAsO_4^{2-}$ and AsO_4^{3-}, especially at a high pH values that may react with Ca^+ as shown by the following equations (Bothe and Brown 1999; Martinez-Villegas et al. 2013):

$$\text{HAsO}_4^{2-} + \text{Ca}^{2+} + n\text{H}_2\text{O} \rightarrow \text{CaHAsO}_4 \cdot n\text{H}_2\text{O} \quad (12)$$

$$2\text{AsO}_4^{3-} + 3\text{Ca}^{2+} + n\text{H}_2\text{O} \rightarrow \text{Ca}_3(\text{AsO}_4)_2 \cdot n\text{H}_2\text{O} \quad (13)$$

However, in real groundwater, the reaction processes follow not only Eq. (11) but also Eqs. (12) and (13). It was found that the efficiency of As removal by Fe-SSS is lower than that by CSS after 10 h in the real groundwater experiment, which is the same as in the synthetic groundwater experiment.

Considering material recycle and reuse, CSS and Fe-SSS were regenerated based on the real groundwater experiment. It is expected that for the conditions studied, the slags were fully regenerated, and increasing the regeneration frequencies would not be expected to have a significant effect on the removal achieved. The results confirm that regeneration of Fe-SSS was achieved compared with CSS. The regeneration experiment found that

As-saturated Fe-SSS performed better than CSS for regeneration. The best regeneration condition is high-temperature treatment at 300 °C for 60 min because high-temperature regeneration provides a sufficient amount of thermal energy to break the adsorbent–adsorbate interactions across all the adsorption sites without degrading the adsorbates (Salvador et al. 2015). This study did not explore other regeneration methods, and this will be the subject of future work.

Table S3 lists a comparison of adsorption capacities of As with different adsorbents. The adsorption capacity of is almost same as the popular adsorbents presented in Table S3. Furthermore, the present CSS and Fe-SSS showed strong neutralization capacity as used in non-neutral environment, and this is an important advantage when using the steel slag instead of other adsorbents for real environmental applications at room temperature. Therefore, the present CSS and Fe-SSS could be considered a promising material for the removal of As from real environment.

Conclusion

This study showed that CSS and Fe-SSS are more efficient substrates for As removal from groundwater than SSS. The modification of SSS by $FeC1_3$ can generate more pore structures and larger surface areas, and the As adsorption capacity of the slag was improved distinctly. The solution pH was a critical parameter for the removal of As for CSS and SSS. CSS, SSS and Fe-SSS could effectively change the solution pH and keep the solution alkaline. The adsorption process was found to follow the pseudo-second-order kinetic model and the Langmuir isotherm model. Thermodynamic studies confirmed that the adsorption process is feasible and spontaneous. It could be concluded that under highly alkaline solution conditions, the mechanism of As removal by CSS and SSS can be attributed to chemisorption, including chemical precipitation and coordination reactions, and under weakly alkaline solution conditions, electrostatic interaction and specific adsorption are the key As removal mechanisms by Fe-SSS. Finally, the experiment confirmed that regeneration of the Fe-SSS was better achieved than that of the other steel slags in the application of high-temperature treatment.

Acknowledgments This research was supported by the Grand Science and Technology Special Project of Shanxi Province (20111101016), the Science & Technology Key Program of Shanxi Province (20140311008-6), Fundamental Research Funds for the Central Universities (SWU116087 and XDJK2017B013) and New Star Foundation on Shaanxi Province Youth Science and Technology (2016KJXX-89).

References

Ahn JS, Chon CM, Moon HS, Kim KW (2003) Arsenic removal using steel manufacturing byproducts as permeable reactive materials in mine tailing containment systems. Water Res 37:2478–2488

Ajmal M, Khan AH, Ahmad S, Ahmad A (1998) Role of sawdust in the removal of copper(II) from industrial wastes. Water Res 32:3085–3091

Asfaram A, Ghaedi M, Agarwal S, Tyagi I, Gupta VK (2015) Removal of basic dye Auramine-O by ZnS: Cu nanoparticles loaded on activated carbon: optimization of parameters using response surface methodology with central composite design. RSC Adv 5:18438–18450

Biswas A, Gustafsson JP, Neidhardt H, Halder D, Kundu AK, Chatterjee D, Berner Z, Bhattacharya P (2014) Role of competing ions in the mobilization of arsenic in groundwater of Bengal Basin: insight from surface complexation modeling. Water Res 55:30–39

Bothe JV, Brown PW (1999) Arsenic immobilization by calcium arsenate formation. Environ Sci Technol 33:3806–3811

Cerkez EB, Bhandari N, Reeder RJ, Strongin DR (2015) Coupled redox transformation of chromate and arsenite on ferrihydrite. Environ Sci Technol 49:2858–2866

Chakrabortty S, Sen M, Pal P (2014) Arsenic removal from contaminated groundwater by membrane-integrated hybrid plant: optimization and control using visual basic platform. Environ Sci Pollut Res 21:3840–3857

Chakraborty A, Sengupta A, Bhadu MK, Pandey A, Mondal A (2014) Efficient removal of arsenic (V) from water using steel-making slag. Water Environ Res 86:524–531

Claveau-Mallet D, Wallace S, Comeau Y (2013) Removal of phosphorus, fluoride and metals from a gypsum mining leachate using steel slag filters. Water Res 47:1512–1520

Dastkhoon M, Ghaedi M, Asfaram A, Goudarzi A, Langroodi SM, Tyagi I, Agarwal S, Gupta VK (2015) Ultrasound assisted adsorption of malachite green dye onto ZnS:Cu-NP-AC: Equilibrium isotherms and kinetic studies—response surface optimization. Sep Purif Technol 156:780–788

Donmez M, Camci S, Akbal F, Yagan M (2015) Adsorption of copper from aqueous solution onto natural sepiolite: equilibrium, kinetics, thermodynamics, and regeneration studies. Desalin Water Treat 54:2868–2882

Duan JM, Su B (2014) Removal characteristics of Cd(II) from acidic aqueous solution by modified steel-making slag. Chem Eng J 246:160–167

Dutre V, Vandecasteele C (1998) Immobilization mechanism of arsenic in waste solidified using cement and lime. Environ Sci Technol 32:2782–2787

Essandoh M, Wolgemuth D, Pittman C, Mohan D, Mlsna T (2017) Adsorption of metribuzin from aqueous solution using magnetic and nonmagnetic sustainable low-cost biochar adsorbents. Environ Sci Pollut Res 24:4577–4590

Freundlich H, Heller W (1939) The Adsorption of cis- and trans-Azobenzene. J Am Chem Soc 61:2228–2230

Grossl PR, Eick M, Sparks DL, Goldberg S, Ainsworth CC (1997) Arsenate and chromate retention mechanisms on goethite. 2. Kinetic evaluation using a pressure-jump relaxation technique. Environ Sci Technol 31:321–326

Gupta VK, Tyagi I, Agarwal S, Sadegh H, Shahryari-ghoshekandi R, Yari M, Yousefi-nejat O (2015) Experimental study of surfaces of hydrogel polymers HEMA, HEMA–EEMA–MA, and PVA as adsorbent for removal of azo dyes from liquid phase. J Mol Liq 206:129–136

Gupta VK, Saravanan R, Agarwal S, Gracia F, Khan MM, Qin J, Mangalaraja RV (2017) Degradation of azo dyes under different wavelengths of UV light with chitosan-SnO_2 nanocomposites. J Mol Liq 232:423–430

Ho YS (2006) Review of second-order models for adsorption systems. J Hazard Mater 136:681–689

Jia Y, Luo T, Yu X, Sun B, Liu JH, Huang XJ (2013) Synthesis of monodispersed alpha-FeOOH nanorods with a high content of surface hydroxyl groups and enhanced ion-exchange properties towards As(V). RSC Adv 3:15805–15811

Kanel SR, Greneche JM, Choi H (2006) Arsenic(V) removal kom groundwater using nano scale zero-valent iron as a colloidal reactive barrier material. Environ Sci Technol 40:2045–2050

Kim YS, Kim DH, Yang JS, Baek K (2012) Adsorption characteristics of As(III) and As(V) on alum sludge from water purification facilities. Sep Sci Technol 47:2211–2217

Lackovic JA, Nikolaidis NP, Dobbs GM (2000) Inorganic arsenic removal by zero-valent iron. Environ Eng Sci 17:29–39

Lagergren S (1898) About the theory of so-called adsorption of soluble substances. Kungliga Svenska Vetenskapsakademiens Handlingar 24:1–39

Langmuir I (1918) The adsorption of gases on plane surfaces of glass, mica and platinum. J Am Chem Soc 40:1361–1403

Luo K, Zhang S, Tian Y, Gao X (2014) Arsenic distribution pattern in different sources of drinking water and their geological background in Guanzhong basin, Shaanxi, China. Acta Geol Sin-English Ed 88:984–994

Martinez-Villegas N, Briones-Gallardo R, Ramos-Leal JA, Avalos-Borja M, Castanon-Sandoval AD, Razo-Flores E, Villalobos M (2013) Arsenic mobility controlled by solid calcium arsenates: a case study in Mexico showcasing a potentially widespread environmental problem. Environ Pollut 176:114–122

Nekouei F, Nekouei S, Tyagi I, Gupta VK (2015) Kinetic, thermodynamic and isotherm studies for acid blue 129 removal from liquids using copper oxide nanoparticle-modified activated carbon as a novel adsorbent. J Mol Liq 201:124–133

Nikfar E, Dehghani MH, Mahvi AH, Rastkari N, Asif M, Tyagi I, Agarwal S, Gupta VK (2016) Removal of Bisphenol A from aqueous solutions using ultrasonic waves and hydrogen peroxide. J Mol Liq 213:332–338

Oh C, Rhee S, Oh M, Park J (2012) Removal characteristics of As(III) and As(V) from acidic aqueous solution by steel making slag. J Hazard Mater 213–214:147–155

Rajendran S, Khan MM, Gracia F, Qin J, Gupta VK, Arumainathan S (2016) Ce^{3+}-ion-induced visible-light photocatalytic degradation and electrochemical activity of ZnO/CeO_2 nanocomposite. Sci Rep 6:31641

Robati D, Mirza B, Rajabi M, Moradi O, Tyagi I, Agarwal S, Gupta VK (2016) Removal of hazardous dyes-BR 12 and methyl orange using graphene oxide as an adsorbent from aqueous phase. Chem Eng J 284:687–697

Salvador F, Martin-Sanchez N, Sanchez-Hernandez R, Sanchez-Montero MJ, Izquierdo C (2015) Regeneration of carbonaceous adsorbents. Part I: thermal regeneration. Microporous Mesoporous Mater 202:259–276

Saravanan R, Shankar H, Prakash T, Narayanan V, Stephen A (2011) ZnO/CdO composite nanorods for photocatalytic degradation of methylene blue under visible light. Mater Chem Phys 125:277–280

Saravanan R, Gupta VK, Narayanan V, Stephen A (2013a) Comparative study on photocatalytic activity of ZnO prepared by different methods. J Mol Liq 181:133–141

Saravanan R, Karthikeyan N, Gupta VK, Thirumal E, Thangadurai P, Narayanan V, Stephen A (2013b) ZnO/Ag nanocomposite: an efficient catalyst for degradation studies of textile effluents under visible light. Mater Sci Eng C 33:2235–2244

Saravanan R, Karthikeyan S, Gupta VK, Sekaran G, Narayanan V, Stephen A (2013c) Enhanced photocatalytic activity of ZnO/CuO nanocomposite for the degradation of textile dye on visible light illumination. Mater Sci Eng C 33:91–98

Saravanan R, Gupta VK, Narayanan V, Stephen A (2014) Visible light degradation of textile effluent using novel catalyst ZnO/γ-Mn2O3. J Taiwan Inst Chem E 45:1910–1917

Saravanan R, Khan MM, Gupta VK, Mosquera E, Gracia F, Narayanan V, Stephen A (2015) ZnO/Ag/Mn_2O_3 nanocomposite for visible light-induced industrial textile effluent degradation, uric acid and ascorbic acid sensing and antimicrobial activity. RSC Adv 5:34645–34651

Sun YK, Zhou GM, Xiong XM, Guan XH, Li LN, Bao HL (2013) Enhanced arsenite removal from water by Ti(SO_4)(2) coagulation. Water Res 47:4340–4348

USEPA (1992) Toxicity characteristic leaching procedure. Method 1311. Office of Solid Waste, Washington, DC

Wang YX, Guo HM, Yan SL, Li YL (2004) Geochemical evolution of shallow groundwater systems and their vulnerability to contaminants: a case study at Datong Basin, Shanxi Province, China. Science Press, Beijing

Weber W, Morris J (1963) Kinetics of adsorption on carbon from solution. J Sanit Eng Div Am Soc Civ Eng 89:31–60

Wickramasinghe SR, Han BB, Zimbron J, Shen Z, Karim MN (2004) Arsenic removal by coagulation and filtration: comparison of groundwaters from the United States and Bangladesh. Desalination 169:231–244

Yang JS, Kim YS, Park SM, Baek K (2014) Removal of As(III) and As(V) using iron-rich sludge produced from coal mine drainage treatment plant. Environ Sci Pollut Res 21:10878–10889